Talanta 218 (2020) 121172

Contents lists available at ScienceDirect

Talanta

journal homepage: www.elsevier.com/locate/talanta

Eliminating sweet spot in MALDI-MS with hydrophobic ordered structure as target for quantifying biomolecules

Ning Li, Shuzhen Dou, Lei Feng, Qunyan Zhu, Nan Lu*

State Key Laboratory of Supramolecular Structure and Materials, College of Chemistry, Jilin University, Changchun, 130012, PR China

ARTICLE INFO

Keywords:
Sweet spot
MALDI-MS
Biosensor
Reproducibility
Quantification

ABSTRACT

In matrix-assisted laser desorption/ionization mass spectrometry (MALDI-MS), the analyte is usually distributed unevenly throughout the sample spot. The area with aggregated analyte molecules contributing abundant signal, is termed as "sweet spot", which results in poor detection reproducibility and makes it impossible to quantify analytes without internal standards. We proposed a strategy to eliminate sweet spot in MALDI-MS by using a hydrophobic ordered structure as target. The target is fabricated by creating a hydrophobic silicon nanopillar array and subsequently decorating it uniformly with poly(methyl methacrylate) nanodots for capturing analytes. The sweet spot is eliminated by distributing analyte molecules uniformly on this target, and then result in a uniform MS image, which demonstrates an ideal reproducibility. Finally, with the target assisted MALDI-MS as biosensor was suitable to analyze practical sample such as bacitracin A in milk. Horse heart myoglobin and, angiotensin III molecules can be quantified without internal standard using α-cyano-4-hydroxycinnamic acid as matrix. This biosensor presented good linearity, high salts tolerance and high signal-to-noise ratio (up to 271.8), even the 1 mol/L salt concentration. This strategy could provide an alternative for improving the performance of MALDI-MS.

1. Introduction

In matrix-assisted laser desorption/ionization mass spectrometry (MALDI-MS) has been widely applied to analyze biomolecules for its advantages of rapid identification [1–5]. "Drop-dry" method is commonly used for sample preparation in MALDI-MS analysis due to its simplicity and applicability [6–8]. But the quantification analysis in MALDI-MS is usually limited by the poor reproducibility introduced by the unavoidable inhomogeneous distribution of analyte-matrix crystals.

In MALDI-MS analysis, the analyte molecules are usually aggregated unevenly in one sample spot, and the area with aggregated analyte molecules is termed as "sweet spot" because it contributes abundant signal. The sweet spot is introduced by "coffee ring" and the intrinsic heterogeneity of the crystallization [9,10], which reduces the shot-to-shot reproducibility. The coffee ring is caused by the different rates of solvent evaporation and the migration of the analyte molecules, which can be successfully prevented by hindering the flux-driven delivery of the solutes, such as increasing the viscosity of the solution [11], accelerating the evaporation rate of the solvent [12], or forcing the shrinkage of the three phase contact line to move the crystals to the center of the deposition area from the edge [10]. But these methods are either only applicable for certain kinds of analytes or need a specific instrument. Moreover, even if the coffee ring is efficiently suppressed, the sweet spot can still exist due to the intrinsic heterogeneity of the crystallization. The heterogeneity of crystallization is caused by the different crystallization rates on different areas bearing uneven distributed nucleation sites. Fukuyama et al. increased the distribution uniformity of the crystals by increasing the crystallization rate through tuning the interaction between the analyte molecules and the matrix [13]. This strategy works only when the interaction of analyte-matrix is suitable, however, it may take a long time to find or synthesize a suitable matrix for a certain analyte. In addition, the coffee ring cannot be avoided during the preparation process. It is essential to simultaneously eliminate the coffee ring and heterogeneous crystallization for improving the detection reproducibility, even the universal quantification analysis in MALDI-MS. The internal standard method is a candidate for quantification in MALDI-MS analysis because it can reduce the influence from sweet spot [9,14]. However, the molecules as internal standards should be of the similar molecular structures and properties with the analytes. It is impossible to find a universal internal standard for any analytes, which makes this method not applicable for some of the analytes. To tackle the above issue, Kim et al. proposed a temperature-selected MALDI spectra method for quantification by using a specific device according to the proportionality between the analyte-to-matrix

* Corresponding author.
E-mail address: luenan@jlu.edu.cn (N. Lu).

https://doi.org/10.1016/j.talanta.2020.121172
Received 16 February 2020; Received in revised form 14 May 2020; Accepted 18 May 2020
Available online 23 May 2020
0039-9140/ © 2020 Elsevier B.V. All rights reserved.

ion abundance ratio and the analyte-to-matrix ratio [15,16]. Tseng et al. achieved the quantification with MALDI based on the excellent sample-to-sample reproducibility obtained by suppressing crystallization during the drying process using sinapinic acid-directed synthesized gold nanoclusters [17]. Ming-Ren et al. achieved quantification of MALDI-MS by improving the reproducibility using 2,5-dihydroxybenzoic acid-encapsulated magnetic nanoparticles with the seed-layer surface [18]. Nevertheless, the referred methods without internal standards still need specific instruments or matrix, which cannot be widely applied as a universal method for MALDI quantification.

In this work, we eliminate sweet spot by using a hydrophobic ordered silicon (Si) nanopillar array as target, which is uniformly decorated with poly(methyl methacrylate) (PMMA) nanodots for capturing analytes. The target assisted MALDI-MS as biosensor achieve an excellent reproducibility in measurements, and allows for the quantification of analytes without internal standard. Besides, the non-wetting surface makes the target of excellent desalting ability, showing a high signal-to-noise (S/N) value even with high concentration of salts.

2. Experimental details

2.1. Materials

Horse heart myoglobin (MYO, Mw = 16,941), angiotensin III (Mw = 931.1), PMMA (Mw = 97,000), PMMA (Mw = 350,000), polystyrene (PS) spheres, 1H, 1H, 2H, 2H-perfluorodecyltrichlorosilane (FDTS), α-cyano-4-hydroxycinnamic acid (CHCA), trifluoroacetic acid (TFA), and acetonitrile (ACN) were purchased from Sigma-Aldrich. Bacitracin A (Bac A, Mw = 1422.69) was purchased from Aladdin. Analytical reagent grade ethanol, acetone, chloroform and urea were purchased from Beijing Chemical Works. The 6 inch Si wafers (n type (100)) were obtained from GRINM Advanced Materials Co. Ltd., China. All aqueous solutions were prepared using 18 Mohms deionized water by Milli-Q system.

2.2. Fabrication of the target

Si wafer was cut into slides, and cleaned by taking ultrasonic bath in acetone, chloroform, ethanol and ultrapure water subsequently. And then the cleaned slides were immersed into the aqueous solution of NH_3: H_2O_2: H_2O with a volume ratio of 1: 1: 5 and kept at 90 °C for 40 min to obtain hydroxyl. A PMMA layer was prepared on the treated Si slides by spin-coating 7.5% PMMA (Mw = 97,000) at 7000 rpm. Then a monolayer of 600 nm PS spheres was self-assembled on the PMMA covered slide. The Si slide with PS spheres was treated on a reactive ion etching system (Plasmalab Oxford 80 plus (ICP 65) system) to reduce the size of PS spheres and create Si nanopillars. The parameters for reducing the size of PS spheres are as follows: the gas flow of O_2 was 50 sccm, the set pressure was 10 mTorr, the radio frequency (RF) was 30 W, the inductively coupled plasma (ICP) was 100 W, and the etching duration was 6 min. The parameters for creating Si nanopillars are as below: the gas flow of SF_6 and CHF_3 was 6 sccm and 45 sccm respectively, the set pressure was 8 mTorr, the RF was 25 W, the ICP was 100 W, and the etching duration was 8 min. After the etching process, the samples were washed with toluene, acetone, chloroform, ethanol, and pure water in order to remove the residual PS spheres and PMMA. Secondly, the FDTS molecules were assembled on its surface by keeping it in gas phase at 250 °C for 4 h. Finally, a thin layer of PMMA (Mw = 350,000, 1%) was spin-coated on the array with the speed of 7000 rpm and heated at 300 °C for 30 min.

2.3. Sample preparation

15 μL of analyte solution was dropped and kept for 20 min on the target for absorbing analytes, and then the droplet was removed using a filter paper. 2 μL of CHCA (in 50% ACN aqueous solution containing 0.1% TFA) was added on the target and air dried.

2.4. Preparation of Bac A sample

According to the reported method [19], Bac A was dissolved in Milli-Q water with the concentration of 100 μmol/L and stored at 4 °C, and then the stock solution was diluted with milk before use.

2.5. Characterization and measurements

The morphologies of the samples were characterized with a scanning electron microscope (SEM, HITACHI SU8020 field emission scanning electron microscope), and an atomic force microscope (AFM, Dimension 3100, Digital Instruments, Santa Babara, CA). The photomicrographs were taken using an EZ4 Light Microscope, Leica. Contact angle (CA) measurement was performed at room temperature on a drop shape analysis system (DSA 10 MK2, KRÜSS). The target with air-dried samples was mounted on a target plate (MTP 384 polished steel target, Bruker, Karlsruhe, Germany) using double-sided carbon tape. All mass spectra were acquired on a Autoflex speed TOF/TOF mass spectrometer (Bruker Daltonics) by linear positive mode at an accelerating voltage of 20 kV with a 200 Hz pulsed Nd:YAG laser (355 nm). Approximately 500 laser shots were accumulated per analysis with 1000 pulses per shot. For imaging experiments, the regions were chosen with a step size of 150 μm.

3. Results and DISCUSSION

3.1. Fabrication of the target and preparation of samples

The detailed fabrication process and the corresponding characterizations of the target are shown in Fig. 1a–d. Briefly, a Si nanopillar array was firstly created with nanosphere lithography [20], as revealed in Fig. S1, the diameter, height and period of the Si nanopillars are 380, 630 and 600 nm, respectively. And then the Si nanopillar array was modified with FDTS molecules in gas phase, finally, PMMA nanodots were uniformly decorated on the Si nanopillar array by heating a spin-coated PMMA layer on the hydrophobic surface based on the dewetting effect [21,22]. Thus, the target is obtained, as shown in Fig. 1d. Clearly, the Si nanopillars are ordered and there are some dark spots on the tops of the nanopillars, which are generated PMMA nanodots. The morphology of the nanodots is further characterized using AFM, and the statistics details of the PMMA nanodots are provided in Fig. S2. The result indicates that the deviation of the total surface area of PMMA nanodots on each Si nanopillar is small enough to guarantee the uniform distribution of analyte molecules on the target. The CA of the target is 140°, as shown in Fig. 1d, which demonstrates that the target is hydrophobic. According to the CA records from Fig. 1a–c, the hydrophobicity is contributed by the FDTS molecules and the nanopillar array. Although the introduction of the PMMA nanodots could decrease the hydrophobicity [23], the hydrophobicity remains because the exposed FDTS area is still large enough. With this target, MALDI-MS detection was conducted. Fig. 1e illustrates the procedure for preparing the final biosensor using the target. The analyte droplet was kept on the hydrophobic substrate for 20 min, as shown in Fig. 2a. In this process, PMMA is expected to capture analyte molecules from solution based on the hydrophobic-hydrophobic interaction [24]. The capturing ability of PMMA is confirmed by comparing the spectra collected respectively on a hydrophobic Si nanopillar array without and with a PMMA layer. The results clearly demonstrate that the signal of analytes cannot be observed on the target without PMMA, but it is very strong on the target with a PMMA layer (Fig. S3), which demonstrates the PMMA can efficiently capture the hydrophobic analytes. After capturing the analyte molecules from the droplet, the residual droplet was removed with a filter paper by capillary force, as shown in Fig. 2b. No obvious liquids

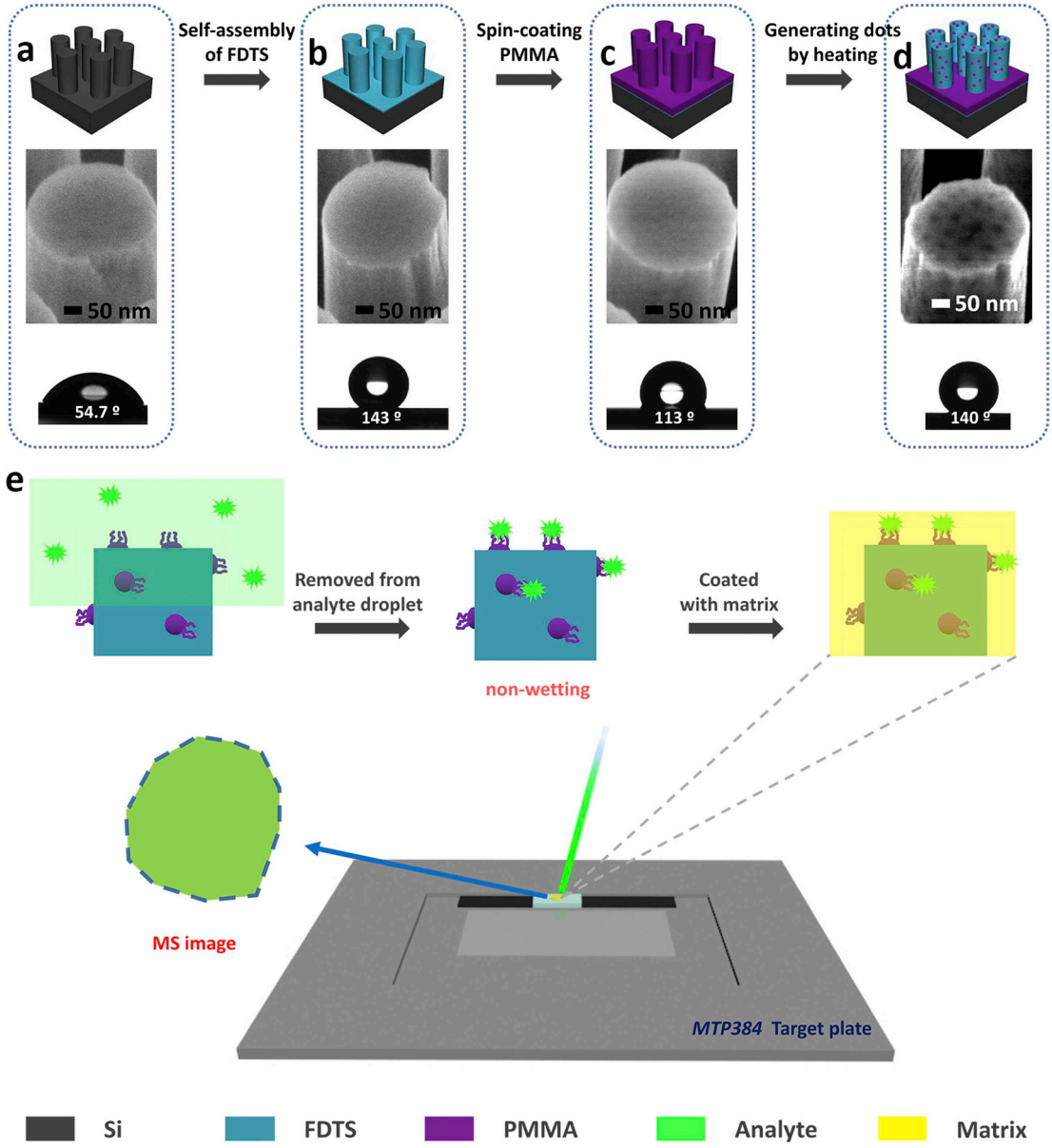

Fig. 1. Fabrication of the target; the corresponding SEM images and CA photographs of (a) Si nanopillar, (b) FDTS modified Si nanopillar, (c) FDTS modified Si nanopillar covered with a PMMA thin layer, and (d) Target. (e) Schematic illustration for preparing the final biosensor using the target.

can be observed because almost no solution can remain on the non-wetting target, which indicates that there is no coffee ring effect, and further confirms the analyte molecules are evenly distributed on the target. The uniform distribution of the analyte molecules should give credit to the ordered Si nanopillars, which promotes the even distribution of PMMA nanodots.

3.2. Optimizing the concentration of the CHCA matrix

CHCA is a widely used matrix for different kinds of molecules due to its high ionization efficiency and signal intensity [25,26]. MYO is a heme protein that can bind small-molecule ligands such as O_2 and CO, and these small molecules are important biological ligands that bind to metalloproteins to function crucially in processes such as signal transduction, respiration and catalysis [27,28]. To find out the suitable amount of matrix for detecting analytes with the proposed method, we applied 2 μL of CHCA with the concentration from 1×10^{-2} to 1×10^{-1} mol/L for testing 1×10^{-5} mol/L of MYO (Fig. S4, Fig. 3a and b). Compared with other concentrations of CHCA, the crystallization of mixture and MS signals are uniform when testing with 8×10^{-2} mol/L of CHCA. The mass spectra of MYO (1×10^{-5} mol/L) and the signal intensity of *m/z* at 16,941 detected with different concentrations of CHCA are shown in Fig. 3c and d. The results demonstrate the signal intensity increases with increasing the concentration of CHCA in the range of 1×10^{-2} to 8×10^{-2} mol/L, but it decreases when further increasing the concentration of CHCA to 1×10^{-1} mol/L. The reason is that too much crystallized CHCA may block the analytes desorption/ionization from the target. Therefore, 8×10^{-2} mol/L of CHCA is applied for detection.

3.3. Quantification of biomolecules without internal standard

MYO (15 μL) was tested as a protein molecule and detected with the concentrations between 1×10^{-7} and 1×10^{-3} mol/L. The signal intensities on the samples were homogeneous on the targets as shows Fig. 4a–e. The data were respectively collected on 100 points, and the

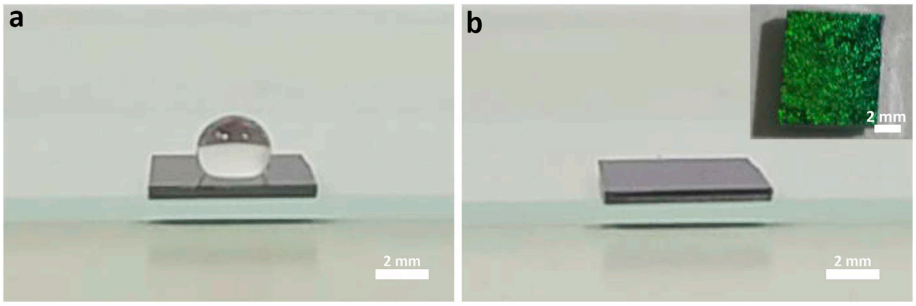

Fig. 2. Photographs of the target (a) before and (b) after removing the droplet of 15 μL of MYO (1×10^{-5} mol/L), the inset is the top view of the sample in b.

average intensities of the mass signals increase with increasing the concentration of MYO, as shown in Fig. 4f. According to the regression equation (1)

$$y = 0.83x + 6.87 \quad (1)$$

the linearity ($R^2 = 0.9552$) is good, as presented in Fig. 4g. Angiotensin III is responsible for stimulating the migration of both androgen-dependent and -independent prostate cancer cell lines [29]. Therefore, angiotensin III, as a peptide, was also tested. As presented in Fig. 5a–e, the intensities of the signals were also homogeneous when detecting angiotensin III (15 μL) of the concentration from 200 to 1000 nmol/L and each data was collected on 50 points for the samples with different concentrations. The average intensities of the signals increase with increasing the concentration of angiotensin III (Fig. 5f). According to the regression equation (2)

$$y = 0.92\,x + 1.31 \quad (2)$$

the linearity ($R^2 = 0.9791$) is also good, as presented in Fig. 5g. To test the method for quantifying analytes in real samples, Bac A in milk with different concentrations was detected. A good linearity ($R^2 = 0.9415$) was obtained as show equation (3).

$$y = 1.19\,x + 9.04 \quad (3)$$

More details are shown in Fig. 6. Furthermore, we compared our method with the previous reported methods based on quantification using MALDI-MS, as shown in Table S1. Even though much more points collected within each sample spot in our strategy than other works, we also acquired good linear results. The above results demonstrate this method is applicable for the quantitative analysis of different molecules without internal standard.

3.4. High salts tolerance

The samples of peptides and proteins always contain salts, but the presence of salts is not favorable for MALDI-MS detection [24,30]. Therefore, an extra desalting step needs to be conducted for the practical applications. With this method, when 15 μL of angiotensin III aqueous solution (1×10^{-6} mol/L) containing 1 mol/L urea was

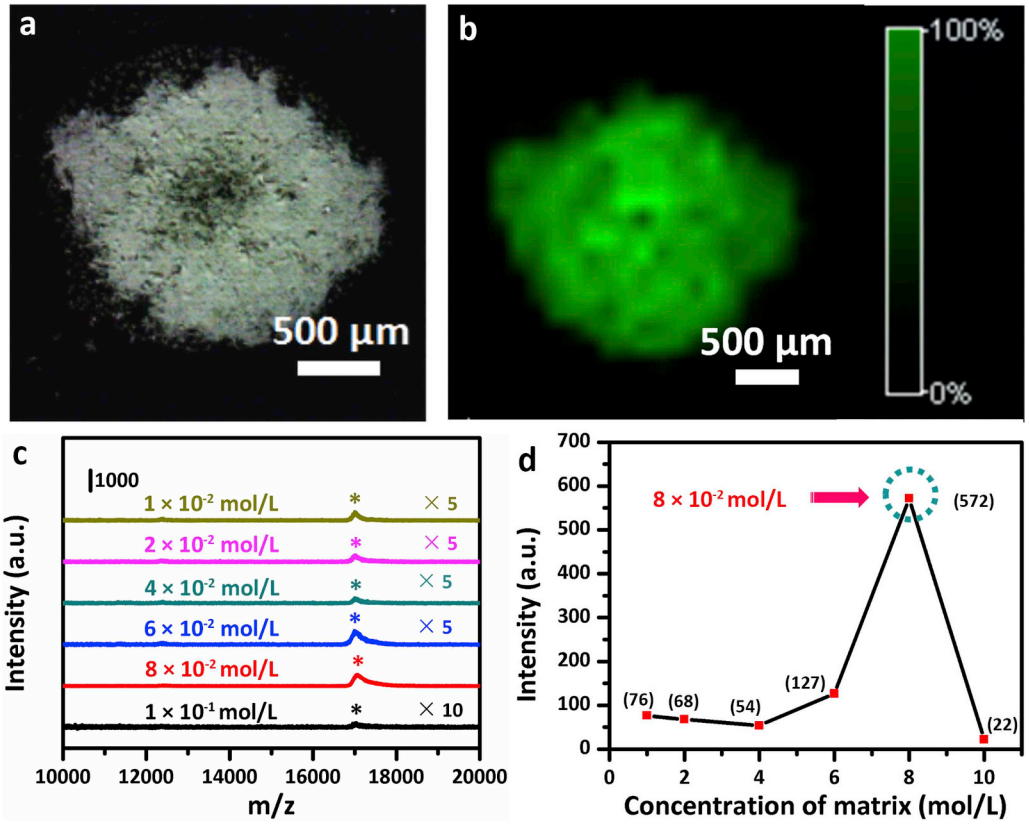

Fig. 3. (a) Photograph and (b) mass image of MYO (1×10^{-5} mol/L) absorbed on the target coated by 2 μL of 8×10^{-2} mol/L CHCA. (c) Average mass spectra of 1×10^{-5} mol/L of MYO (*, *m/z*: 16,941) with CHCA of different concentrations. (d) Statistics of the average peak intensities at 16,941 of MYO (1×10^{-5} mol/μL) detected with CHCA of different concentrations. The values inside the bracket is the measured intensity for MYO with each concentration.

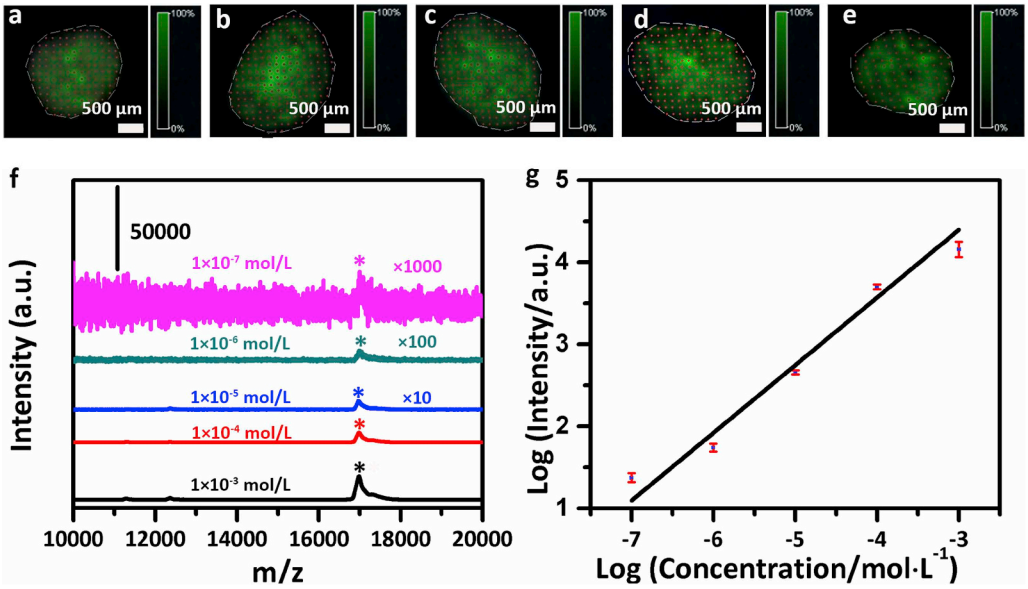

Fig. 4. Mass images of MYO (*, *m/z*: 16,941) with the concentration of (a) 1×10^{-3}, (b) 1×10^{-4}, (c) 1×10^{-5}, (d) 1×10^{-6} and (e) 1×10^{-7} mol/L measured on the target with 2 μL of CHCA (8×10^{-2} mol/L) as matrix. (f) Average mass spectra, and (g) correlation of the intensity and the concentration of MYO in the range of 1×10^{-7} to 1×10^{-3} mol/L with 2 μL of CHCA (8×10^{-2} mol/L) as matrix.

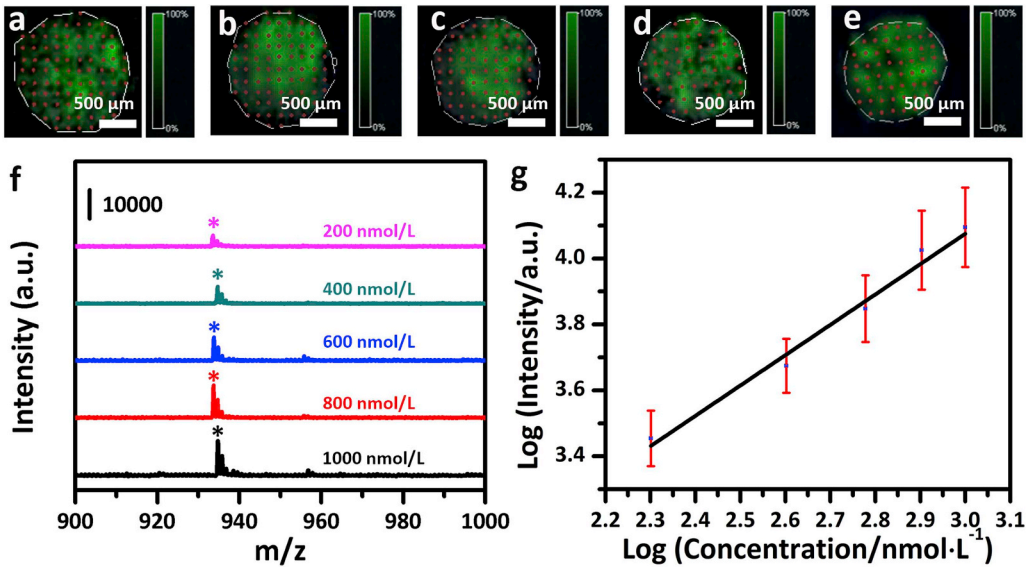

Fig. 5. Mass images of the angiotensin III (*, *m/z*: 931.1) molecules with the concentration of (a) 200, (b) 400, (c) 600, (d) 800 and (e) 1000 nmol/L measured on the target with 2 μL of CHCA (8×10^{-2} mol/L) as matrix. (f) Average mass spectra, and (g) correlation of the intensity and the concentration of angiotensin III in the range of 200 to 1000 nmol/L with 2 μL of CHCA (8×10^{-2} mol/L) as matrix.

dropped and kept on the target for 20 min, as shown in Fig. S5a, no obvious liquids and aggregates can be observed on the target right after the removal of the residual droplet because of the non-wetting surface of the target. Therefore, the salts in solution can hardly remain on the target after removing the residual droplet. The spectra were collected and shown in Fig. S5b, and the S/N is up to 271.8 at the *m/z* of 931.1, which further demonstrates the desalting ability of the target.

4. Conclusions

This work indicates that the target assisted MALDI-MS as biosensor based on Si-PMMA nanodots is applicable for reproducible detection of biomolecules by eliminating sweet spot. Using CHCA as matrix, a good linearity to calibration curve for MYO and angiotensin III was obtained. In addition, this target presents favorable desalting ability, the S/N for detecting angiotensin III was up to 271.8 even with 1 mol/L salt. The success in analysis of real sample such as Bac A in milk makes this idea be a promise, which could be applied for detecting other analytes by designing suitable targets. The strategy could be applied for improving the performance and promoting the applications of MS detection.

CRediT authorship contribution statement

Ning Li: Conceptualization, Methodology, Formal analysis, Investigation, Validation, Visualization, Writing - original draft. **Shuzhen Dou:** Methodology, Formal analysis. **Lei Feng:** Writing - review & editing. **Qunyan Zhu:** Formal analysis. **Nan Lu:** Project administration, Supervision, Writing - review & editing.

Declaration of competing interest

The authors declare that they have no known competing financial interests or personal relationships that could have appeared to influence the work reported in this paper.

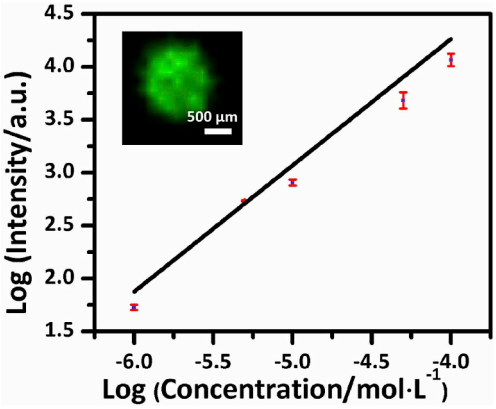

Fig. 6. Correlation of the intensity and the concentration of Bac A in milk in the range of 10^{-6} to 10^{-4} mol/L with 2 μL of CHCA (8×10^{-2} mol/L) as matrix. The inset shows the mass image of Bac A in milk with a concentration of 10^{-4} mol/L.

Acknowledgments

This work was supported by the National Natural Science Foundation of China (No. 21673096).

Appendix A. Supplementary data

Supplementary data to this article can be found online at https://doi.org/10.1016/j.talanta.2020.121172.

References

[1] M. Bertolla, L. Cenci, A. Anesi, E. Ambrosi, F. Tagliaro, L. Vanzetti, G. Guella, A.M. Bossi, Solvent-responsive molecularly imprinted nanogels for targeted protein analysis in MALDI-TOF mass spectrometry, Acs Appl. Mater. Inter. 9 (8) (2017) 6908–6915.
[2] J.J. Hu, F. Liu, H.X. Ju, MALDI-MS patterning of caspase activities and its application in the assessment of drug resistance, Angew. Chem. Int. Ed. 55 (23) (2016) 6666–6669.
[3] J.M. Park, J.I. Kim, H.W. Song, J.Y. Noh, M.J. Kang, J.C. Pyun, Highly sensitive bacterial susceptibility test against penicillin using parylene-matrix chip, Biosens. Bioelectron. 71 (2015) 306–312.
[4] J. Gopal, N. Hasan, H.F. Wu, Fabrication of titanium based MALDI bacterial chips for rapid, sensitive and direct analysis of pathogenic bacteria, Biosens. Bioelectron. 39 (1) (2013) 57–63.
[5] C.H. Lee, J. Gopal, H.F. Wu, Ionic solution and nanoparticle assisted MALDI-MS as bacterial biosensors for rapid analysis of yogurt, Biosens. Bioelectron. 31 (1) (2012) 77–83.
[6] N. AlMasoud, E. Correa, D.K. Trivedi, R. Goodacre, Fractional factorial design of MALDI-TOF-MS sample preparations for the optimized detection of phospholipids and acylglycerols, Anal. Chem. 88 (12) (2016) 6301–6308.
[7] Y. Fukuyama, S. Izumi, K. Tanaka, 3-Hydroxy-4-nitrobenzoic acid as a MALDI matrix for in-source decay, Anal. Chem. 88 (16) (2016) 8058–8063.
[8] L. Blanc, A. Lenaerts, V. Dartois, B. Prideaux, Visualization of Mycobacterial Biomarkers and Tuberculosis Drugs in Infected Tissue by MALDI-MS Imaging, Anal. Chem. 90 (10) (2018) 6275–6282.
[9] Y.B. Wei, S.M. Li, J.X. Wang, C.Y. Shu, J.A. Liu, S.X. Xiong, J.W. Song, J.J. Zhang, Z.W. Zhao, Polystyrene spheres-assisted matrix-assisted laser desorption ionization mass spectrometry for quantitative analysis of plasma lysophosphatidylcholines, Anal. Chem. 85 (9) (2013) 4729–4734.
[10] O. Kudina, B. Eral, F. Mugele, e-MALDI: An electrowetting-enhanced drop drying method for MALDI mass spectrometry, Anal. Chem. 88 (9) (2016) 4669–4675.
[11] Y. Kim, G.B. Hurst, M.J. Doktycz, M.V. Buchanan, Improving spot homogeneity by using polymer substrates in matrix-assisted laser desorption/ionization mass spectrometry of oligonucleotides, Anal. Chem. 73 (11) (2001) 2617–2624.
[12] J. Preisler, P. Hu, T. Rejtar, B.L. Karger, Capillary electrophoresis-matrix-assisted laser desorption/ionization time-of-flight mass spectrometry using a vacuum deposition interface, Anal. Chem. 72 (20) (2000) 4785–4795.
[13] Y. Fukuyama, C. Nakajima, S. Izumi, K. Tanaka, Membrane protein analyses using alkylated trihydroxyacetophenone (ATHAP) as a MALDI matrix, Anal. Chem. 88 (3) (2016) 1688–1695.
[14] C.W. Chumbley, M.L. Reyzer, J.L. Allen, G.A. Marriner, L.E. Via, C.E. Barry, R.M. Caprioli, Absolute quantitative MALDI imaging mass spectrometry: a case of rifampicin in liver tissues (vol 88, pg 2392, Anal. Chem. 88 (17) (2016) 2016) 8920-8920.
[15] K.M. Park, Y.J. Bae, S.H. Ahn, M.S. Kim, A simple method for quantification of peptides and proteins by matrix-assisted laser desorption ionization mass spectrometry, Anal. Chem. 84 (23) (2012) 10332–10337.
[16] S.H. Ahn, T. Hyeon, M.S. Kim, J.H. Moon, Gain switching for a detection system to accommodate a newly developed MALDI-based quantification method, J. Am. Soc. Mass Spectrom. 28 (9) (2017) 1987–1990.
[17] T.H. Chen, C.J. Yu, W.L. Tseng, Sinapinic acid-directed synthesis of gold nanoclusters and their application to quantitative matrix-assisted laser desorption/ionization mass spectrometry, Nanoscale 6 (3) (2014) 1347–1353.
[18] Y.C. Ho, M.C. Tseng, Y.W. Lu, C.C. Lin, Y.J. Chen, M.R. Fuh, Nanoparticle-assisted MALDI-TOF MS combined with seed-layer surface preparation for quantification of small molecules, Anal. Chim. Acta 697 (1–2) (2011) 1–7.
[19] X.Y. Wang, N. Li, D.R. Xu, X.C. Yang, Q.Y. Zhu, D.Y. Xiao, N. Lu, Superhydrophobic candle soot/PDMS substrate for one-step enrichment and desalting of peptides in MALDI MS analysis, Talanta 190 (2018) 23–29.
[20] H.B. Xu, N. Lu, D.P. Qi, J.Y. Hao, L.G. Gao, B. Zhang, L.F. Chi, Biomimetic antireflective Si nanopillar arrays, Small 4 (11) (2008) 1972–1975.
[21] D. Gentili, G. Foschi, F. Valle, M. Cavallini, F. Biscarini, Applications of dewetting in micro and nanotechnology, Chem. Soc. Rev. 41 (12) (2012) 4430–4443.
[22] Y.J. Oh, C.A. Ross, Y.S. Jung, Y. Wang, C.V. Thompson, Cobalt nanoparticle arrays made by templated solid-state dewetting, Small 5 (7) (2009) 860–865.
[23] J.H. Wang, W.M. Zhou, J. Zhang, M.J. Yang, C.T. Ji, X.X. Shao, L.Y. Shi, High-fidelity replica molding for large-area PMMA 3D nanostructures with high performance surface-enhanced Raman scattering and hydrophobicity, Microelectron. Eng. 115 (2014) 2–5.
[24] Z.F. Zeng, Y.D. Wang, S.L. Shi, L.F. Wang, X.H. Guo, N. Lu, On-plate selective enrichment and self-desalting of peptides/proteins for direct MALDI MS analysis, Anal. Chem. 84 (5) (2012) 2118–2123.
[25] H.M. Chen, C.H. Deng, X.M. Zhang, Synthesis of Fe3O4@SiO2@PMMA core-shell-shell magnetic microspheres for highly efficient enrichment of peptides and proteins for MALDI-ToF MS analysis, Angew. Chem. Int. Ed. 49 (3) (2010) 607–611.
[26] H.M. Xiong, X.Y. Guan, L.H. Jin, W.W. Shen, H.J. Lu, Y.Y. Xia, Surfactant-free synthesis of SnO2@PMMA and TiO2@PMMA core-shell nanobeads designed for peptide/protein enrichment and MALDI-TOF MS analysis, Angew. Chem. Int. Ed. 47 (22) (2008) 4204–4207.
[27] K.Y. Oang, K.H. Kim, J. Jo, Y.M. Kim, J.G. Kim, T.W. Kim, S. Jun, J. Kim, H. Ihee, Sub-100-ps structural dynamics of horse heart myoglobin probed by time-resolved X-ray solution scattering, Chem. Phys. 442 (2014) 137–142.
[28] K. Chu, J. Vojtchovsky, B.H. McMahon, R.M. Sweet, J. Berendzen, I. Schlichting, Structure of a ligand-binding intermediate in wild-type carbonmonoxy myoglobin, Nature 403 (6772) (2000) 921–923.
[29] K. Dominska, A.W. Piastowska-Ciesielska, A. Lachowicz-Ochedalska, T. Ochedalski, Similarities and differences between effects of angiotensin III and angiotensin II on human prostate cancer cell migration and proliferation, Peptides 37 (2) (2012) 200–206.
[30] W.T. Jia, X.H. Chen, H.J. Lu, P.Y. Yang, CaCO3-poly(methyl methacrylate) nanoparticles for fast enrichment of low-abundance peptides followed by CaCO3-core removal for MALDI-TOF MS analysis, Angew. Chem. Int. Ed. 45 (20) (2006) 3345–3349.